Journal of Integrative Agriculture 2026, 25(8): 3126–3138

Available online at ScienceDirect

Journal of Integrative Agriculture



RESEARCH ARTICLE

Identification and validation of two QTLs associated with Fusarium head blight resistance in spring wheat (*Triticum aestivum* L.)

Cong Li[2, 3*], Lei Wu[1*], Xinyao He[2], Yi He[1], Peng Jiang[1], Jian Ma[3], Pawan K. Singh[2#], Xu Zhang[1, 4#]

[1] *CIMMYT-JAAS Joint Center for Wheat Diseases, Jiangsu Academy of Agricultural Sciences, Nanjing 210014, China*
[2] *International Maize and Wheat Improvement Center, Texcoco C.P. 56237, Mexico*
[3] *State Key Laboratory of Crop Gene Exploration and Utilization in Southwest China/Triticeae Research Institute, Sichuan Agricultural University, Chengdu 611130, China*
[4] *Collaborative Innovation Center for Modern Crop Production Co-sponsored by Jiangsu Province and Ministry of Agriculture and Rural Affairs, Nanjing 210095, China*

Highlights

- New major quantitative trait loci for Fusarium head blight (FHB) resistance were detected.
- Stacking above QTL markedly increased resistance against both FHB and deoxynivalenol (DON).

Abstract

Fusarium head blight (FHB) is one of the most important and destructive wheat diseases worldwide, threatening both food security and safety. In this study, a recombinant inbred line (RIL) population with 269 F_6 lines developed from a cross between 'Nanjing 8611' and 'Ocoroni' was used to map quantitative trait loci (QTLs) for FHB resistance. Field FHB trials were conducted for three years in Nanjing, China, using point inoculation, and two years in Mexico with spray inoculation. A high-density genetic map was constructed for the RIL population using the wheat 55 K single nucleotide polymorphism (SNP) array. A total of 13 QTLs were detected on chromosomes 1B, 2D, 3B, 5D, 6D, and 7A, among which two major QTLs, *QFhb.CIM-2D.1* and *QDon.CIM-3B.1*, were stably expressed in this study. Conditional QTL analysis suggested that *QFhb.CIM-2D.1* contributes to reduced deoxynivalenol (DON) content *via* decreasing FHB severity, whereas *QDon.CIM-3B.1* contributed to FHB resistance by directly controlling DON accumulation. Stacking of *QFhb.CIM-2D.1* and *QDon.CIM-3B.1* exhibited a marked increase in resistance against both FHB and DON. Furthermore, two Kompetitive Allele-Specific PCR (KASP) markers, *KASP-1369* and *KASP-8394*, tightly linked to *QFhb.CIM-2D.1* and *QDon.CIM-3B.1*, respectively, were developed and successfully validated in their respective genetic populations. Altogether, these results broaden the understanding of the genetic basis of resistance to FHB, and the developed markers are valuable for marker-assisted wheat breeding.

Keywords: wheat, Fusarium head blight, QTL mapping, deoxynivalenol (DON), disease resistance

1. Introduction

Bread wheat (*Triticum aestivum* L.) is one of the important cereal crops in the world, and its production has frequently been challenged by diseases that significantly affect the yield and quality of wheat (Awika 2011; McIntosh 1998). Fusarium head blight (FHB) is a major wheat disease that has its epidemic regions mainly in East Asia, the Americas, and Europe (Ma *et al.* 2020). With changes in climate and wheat cultivation strategies, the disease is becoming more severe in many other regions, a good example is Ethiopia, where FHB caused severe yield losses of up to 100% in the last few years (Mengesha *et al.* 2022). FHB is mainly caused by *Fusarium graminearum* species complex and can cause significant yield losses globally (Bai *et al.* 2018). For instance, FHB normally causes yield losses of 5 to 10% in

Received 5 August 2024; Received in revised form 29 September 2024; Accepted 22 October 2024; Available online 18 December 2024
Cong Li, E-mail: licong20210317@163.com; #Correspondence Pawan K. Singh, E-mail: pk.singh@cgiar.org; Xu Zhang, Tel: +86-25-84390293, Fax: +86-25-84390321, E-mail: xuzhang@jaas.ac.cn
* These authors contributed equally to this study.

© 2026 CAAS. Publishing services by Elsevier B.V. on behalf of KeAi Communications Co. Ltd. This is an open access article under the CC BY-NC-ND license (http://creativecommons.org/licenses/by-nc-nd/4.0/). Peer review under responsibility of Editorial Board of *Journal of Integrative Agriculture*.
doi: 10.1016/j.jia.2024.12.021

China, but during severe epidemics, the losses can exceed 30% and reach 100% (Cheng *et al.* 2012). Furthermore, a range of mycotoxins, especially deoxynivalenol (DON), are produced during FHB infection, contaminating wheat grains and threatening human and animal health (Miller *et al.* 1997). Under heavy FHB infection, grains could have too high DON contamination to be harvested, e.g., approximately 18% of the wheat area was not harvested in 1994 in northwestern Minnesota (McMullen *et al.* 1997).

Varietal resistance against FHB has been regarded as an indispensable component in the FHB management system. Based on host response to pathogen infection, several types of resistance were observed, including resistance to initial pathogen penetration (type I), to the spread of pathogen in spike tissues (type II), and to mycotoxin accumulation (type III) (Bai *et al.* 2018). Numerous quantitative trait loci (QTLs) have been associated with individual or multiple types of FHB resistance (Zheng *et al.* 2021; Chen *et al.* 2022). For example, a QTL on chromosome 2B was associated with type I resistance (Gilsinger *et al.* 2005), a QTL on chromosome 3B that corresponds to *Fhb1* was associated with type II resistance (Su *et al.* 2018), and a QTL on chromosome 5A was primarily associated with low DON content (Ma *et al.* 2006). A QTL on 2DLc was associated with types I and III resistance (He *et al.* 2016a). However, some QTLs for FHB resistance are linked to undesirable agronomic traits, such as tall stature and late heading, limiting their utilization in wheat breeding (Xu *et al.* 2023).

Due to the lack of resistant sources and the complexity of resistance mechanisms, only seven genes imparting resistance to FHB have been formally designated, with only two, *Fhb1* and *Fhb7*, having been cloned (Zheng *et al.* 2021). Both *Fhb1* (3BS) and *Fhb2* (6BS) were derived from 'Sumai 3', and the former has been utilized in global wheat breeding programs aimed at enhancing FHB resistance. *Fhb4* (4BL) and *Fhb5* (5AS) are among the most effective type I resistance QTLs and were derived from the Chinese landrace 'Wangshuibai' (Xue *et al.* 2011). The remaining *Fhb* genes are from wild relatives of wheat, i.e., *Fhb3* was derived from *Leymus racemosus* (Qi *et al.* 2008), *Fhb6* from *Elymus tsukushiensis* (Cainong *et al.* 2015), and *Fhb7* from *Thinopyrum elongatum* (Wang *et al.* 2020). Additional QTLs or Meta-QTLs for FHB resistance have been identified on all 21 wheat chromosomes with various phenotypic effects (Zheng *et al.* 2021), further demonstrating the complexity of FHB resistance in wheat.

In our previous studies conducted in Mexico, a Chinese spring wheat line 'Nanjing 8611' exhibited desirable agronomic traits and resistance against a broad spectrum of diseases, including FHB (He *et al.* 2014; Osman *et al.* 2016). A recombinant inbred line (RIL) population was thus developed using 'Nanjing 8611' and 'Ocoroni' to dissect genetic factors underlying resistance to the diseases. In this study, the population was evaluated for FHB resistance in both Mexico and China to identify consistent QTLs and their flanking markers, which were evaluated in additional genetic populations for their usefulness in marker-assisted selection.

2. Materials and methods

2.1. Plant materials

A RIL population with 269 F_6 lines derived from a cross between 'Nanjing 8611' and 'Ocoroni' (referred to as NJO hereafter) was used to identify QTL for FHB resistance. The female parent 'Nanjing 8611' with good FHB resistance is a spring wheat genotype introduced from Jiangsu, China, in 1988, with a pedigree of NING-7084/YANGMAI-3//XIAO-JIAN-42 (https://www.genesys-pgr.org/10.18730/BAW92), whereas the male parent 'Ocoroni' (moderately susceptible to FHB) is an International Maize and Wheat Improvement Center (CIMMYT) spring wheat line with a pedigree of JUPATECO F 73/EMU//GRAJO (https://www.genesys-pgr.org/10.18730/BCCW3). Additionally, two different genetic populations were used for validation of the major QTLs identified in the current study, including a doubled haploid population (referred to as DH) developed through hybridizing 'TRAP#1/BOW//Taigu derivative' with 'Ocoroni' (He *et al.* 2016b), and a spring wheat panel (referred to as SWP) including 256 wheat lines of global origin (Wu *et al.* 2022). FHB and DON data of the two validation populations reported in the respective studies were used in the current study to associate marker alleles with FHB/DON resistance. The DH population was evaluated only in Mexico (He *et al.* 2016b), whereas the SWP population was evaluated in both Mexico and China (Wu *et al.* 2022).

2.2. Phenotypic evaluation

The NJO population was evaluated in the El Batan Station of CIMMYT, Mexico, during the 2018–2019 (2019-M) and 2020–2021 (2021-M) growing seasons; it was then evaluated in Nanjing, Jiangsu Province, China, during the 2019–2020 (2020-NJ), 2020–2021 (2021-NJ), and 2021–2022 (2022-NJ) growing seasons. In each field experiment, the RILs and their parents were planted in plots with two replications. Each plot consisted of two 1.0-m row spaced 0.30 m apart with 30 seeds per row. Field management followed the local standard practices.

In Mexico, an inoculum prepared from a mixture of five *F. graminearum* isolates, including CIMFU No. 85, 89, 108, 162, and 222, was used to inoculate wheat spikes according to the protocols described by He *et al.* (2013). These isolates were obtained from naturally infected wheat heads at the El Batan station in 2017 and selected for their high DON productivity and aggressiveness in greenhouse experiments. At anthesis, the field plots were sprayed with an inoculum of 50,000 spores mL^{-1}, and the procedure was repeated 2 d later to reinforce the infection. A misting system was set up in the nursery, operational from 9 a.m. to 8 p.m. with 10 min of spraying each hour to maintain a humid environment conducive to FHB infection. Field evaluation of FHB infection was conducted at 25 days post-inoculation on the 10 spikes marked with different tags at anthesis to evaluate the mixed effects of type I and type II resistance (Wu *et al.* 2022). Each line was scored for the calculation of the FHB index with the formula: FHB index=Severity (the averaged percentage of diseased spikelet)×Incidence (the percentage of symptomatic spikes) according to the previous

studies (He *et al.* 2019; Wu *et al.* 2022). After harvest, a 20-g grain sample was finely ground utilizing a coffee mill, and a 2-g subsample was taken for DON quantification using the DON Enzyme-linked Immunosorbent Assay (ELISA) Kit (RBiopharm GmbH, Darmstadt, Germany), following the manufacturer's instructions (He *et al.* 2019). Besides, plant height (PH) was measured from the base of the plant to the top of the main spike, excluding awns (Li *et al.* 2020). Days to heading (DTH) were calculated from the planting to the date when half of the plants in a given plot reached anthesis (He *et al.* 2016a).

In China, *F. asiaticum* isolates Fa0609, Fa1312, and Fa0980 from Jiangsu Academy of Agricultural Sciences (Nanjing, China) were used in this study. Point inoculation was conducted, where 10 spikes per line were inoculated by injecting 10 μL suspension of *F. asiaticum* (100,000 spores mL^{-1}) into a central spikelet at anthesis. Subsequently, the inoculated spikes were covered with a plastic bag for 3 d to maintain optimal moisture conditions for fungal infection (Wu *et al.* 2022). FHB severity was assessed by recording the number of diseased spikelets on the 21st d post-inoculation, and then the inoculated spikes were harvested to detect DON content with the DON ELISA Test Kit following the manufacturer's instructions (Huaan Magnech Bio-tech, China) (Wu *et al.* 2022).

2.3. Genetic map construction

Genomic DNA was extracted from young leaf samples following the cetyltrimethyl ammonium bromide (CTAB) method, and DNA integrity and quantity were subsequently checked with a ND1000 spectrophotometer (Thermo Fisher Scientific Inc., Waltham, MA, USA). Genotyping was performed using a wheat 55 K SNP array at CapitalBio Technology (Beijing, China). Markers with a minor allele frequency of less than 30% and segregation ratio beyond the range of 0.5–2.0 were discarded, and the remaining markers were analyzed for redundancy using the BIN function of IciMapping 4.1 (http://www.isbreeding.net/). The groups of bin markers were ordered in JoinMap 4.0 using the Kosambi mapping function with LOD values ranging from 5 to 30, and MapChart 2.2 (http://www.biometris.nl/uk/Software/MapChart/) was used to draw genetic maps (Liu *et al.* 2018). Marker sequences were blasted against the IWGSC RefSeq v1.1 (http://www.wheatgenome.org/) to retrieve physical locations. The collinearity between the genetic and the physical maps was further compared and analyzed using Excel (version 2016) and Origin 2021 software (https://www.originlab.com).

2.4. QTL analysis

QTL mapping was performed on best linear unbiased prediction (BLUP) datasets from Mexico (BLUP-M) and Nanjing (BLUP-NJ), using the MapQTL 6.0 software package (https://www.kyazma.nl/index.php/MapQTL/) with the multiple QTL model mapping (MQM) algorithm with LOD score values≥3.40 calculated by 1,000-permutation tests model (Van Ooijen 2009). The multi-environment traits (MET) algorithm of IciMapping 4.1 was used to confirm the stable QTL identified by MQM. QTL names were assigned according to the rules of the International Rules of Genetic Nomenclature (http://wheat.pw.usda.gov/ggpages/wgc/98/Intro.htm), with 'Fhb' and 'CIM' standing for 'Fusarium head blight' and 'CIMMYT', respectively.

2.5. Conditional QTL analysis

QGAStation2.0 software (Zhu 1995; Cui *et al.* 2011) was used to calculate the conditional phenotypic values (e.g., DON|FHB), and the complex relationship between the FHB index and DON content was then evaluated using closely linked flank markers.

2.6. Marker development and QTL validation

Two KASP markers, *KASP-1369* and *KASP-8394*, were developed to validate the newly identified QTLs on chromosomes 2DS and 3BS, respectively. Ninety lines randomly selected from the DH population were used to validate the stable QTLs on chromosome 2DS using *KASP-1369* marker (*KASP-1369*F_1: gaaggtgaccaagttcatgctCGGACTGAAAAGATGCGCA, *KASP-1369*F_2: gaaggtcggagtcaacggattCGGA CTGAAAAGAT GCGCG, *KASP-1369*R: TCTTCAGTCTTGCGCTTC), and the 256 genotypes of SWP were used to validate the major QTLs on chromosomes 2DS and 3BS utilizing *KASP-1369* and *KASP-8394*, respectively (*KASP-8394*F_1, gaaggtcggagtcaacggattGTAGTACTTTATAGGTCCAC; *KASP-8394*F_2, gaaggtgaccaagttcatgctGTAGTACTTTATAGGTCCAG; *KASP-8394*R, CTATATATGGTCCACCTTTGAC). KASP genotyping was performed on the CFX96™ Real-Time PCR System (Bio-Rad Laboratories, Hercules, CA, USA). The amplification reactions were performed in a total volume of 10 μL per sample, containing 5 μL of template DNA (50 ng μL^{-1}), 5 μL of Mix buffer with a total volume of 0.138 μL mixture primers (100 μmol L^{-1}), and 4.862 μL PACE Genotyping Master Mix (3CR Bioscience Ltd., Essex, UK). The PCR reaction procedure was as follows: firstly, 15 min at 94°C; then 10 cycles of 20 s at 94°C, and 60 s at 65°C–57°C (touchdown –0.8°C per cycle); subsequently, 35 cycles of 20 s at 94°C, and 60 s at 57°C.

Besides, the diagnostic marker *TaHRC* (F: ATTCCTACTAGCCGCCTGGT; R: ACTGGGGCAAGCAAACATTG) was used to confirm the absence of *Fhb1* in the two parents of the NJO population, following the protocols in Su *et al.* (2018).

2.7. Candidate gene prediction and database mining

Candidate genes for the major QTLs identified in the current study were obtained from WheatOmics 1.0 (Ma *et al.* 2021), and their annotations and functions were further analyzed using UniProt (https://www.uniprot.org/). Furthermore, the physical locations of the flanking markers of the QTL in IWGSC RefSeq v2.1 (http://wheatgenome.org), Kenong 9204 genome (Shi *et al.* 2022), wild emmer genome v.2.0 (Zhu *et al.* 2019a), and *Aegilops tauschii* (AY17) genome (Zhou *et al.* 2021) were obtained *via* BLAST searches. Collinearity of the two major QTLs between the genetic and physical maps was compared and visualized using Origin (2021

version) software. Expression patterns of the candidate genes in spike and grain were obtained from the wheat expression database of Chinese Spring Development (pair) in WheatOmics 1.0 (Ma *et al.* 2021), as well as from Wheat Expression Browser (powered by expVIP, http://www.wheat-expression.com/).

2.8. Data analysis

The MIXED procedure of SAS V8.0 software (SAS Institute, Cary, NC, USA; https://www.sas.com) was used to calculate the BLUP values of target traits (FHB, DON, PH, and DTH) across environments (Smith *et al.* 1998). Analysis of variance (ANOVA) was performed with the PROC GLM module in SAS V8.0. IBM SPSS Statistics 26 (SPSS, Chicago, IL, USA; https://en.wikipedia.org/wiki/SPSS) was used to perform Student's *t*-test (P<0.05) and correlation analysis (Li *et al.* 2020). Origin 2021 software was used to draw quantile-quantile (Q-Q) plots and boxplots.

3. Results

3.1. Phenotypic evaluation

Significant differences in FHB resistance were observed between the two parents, 'Nanjing 8611' and 'Ocoroni', where the former performed consistently better than the latter (Fig. 1). RIL lines of the NJO population exhibited a continuous distribution in FHB (Fig. 1) and DON (Appendix A), and there are lines displaying transgressive segregation. Disease pressure in the two years in Mexico was comparable, with 2021-M having a slightly higher infection rate than 2019-M.

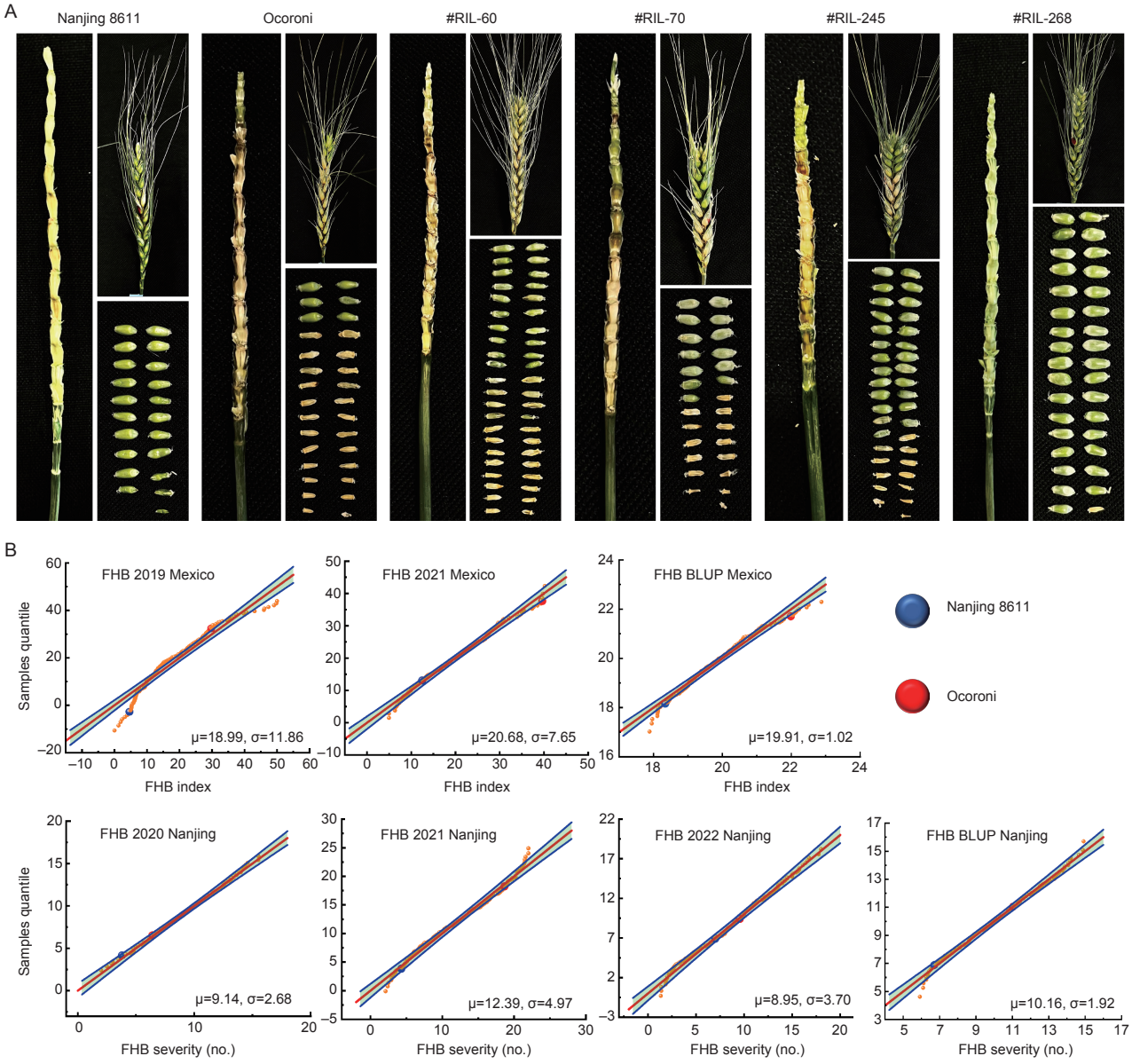


Fig. 1 Phenotypic variation of the parents and recombinant inbred line (RIL) lines of the 'Nanjing 8611' and 'Ocoroni' F_6 (NJO) population. A, Fusarium head blight (FHB) symptoms of the parents, 'Nanjing 8611' and 'Ocoroni', and selected lines with different levels of resistance. B, quantile-quantile (Q-Q) plots for the distribution of FHB in different environments.

As for the experiments in Nanjing, 2021-NJ exhibited much higher infection than the other two experiments (Table 1). The DON levels in Nanjing are consistently higher than those in Mexico, with a higher standard deviation (SD) as well (Table 1; Appendix A). PH and DTH displayed wide ranges in Mexico (Table 1), and both exhibited normal distribution (Appendix A). ANOVA demonstrated the significant effects of 'genotype', as well as of 'genotype-by-environment interaction' (Appendix B).

Significant and positive correlations (P<0.01) were detected between FHB and DON, with correlation coefficient of 0.512 in Mexico and 0.635 in Nanjing; however, a relatively low correlation (r=0.26) for FHB between the two locations was observed, reflecting the different resistance types measured (Table 2). Low correlation was observed between FHB/DON and DTH/PH in Mexico (Table 2).

3.2. Genetic map construction and comparison with physical maps

A total of 3,569 non-redundant markers were used for linkage analysis and map construction, yielding 28 linkage groups across the 21 chromosomes in wheat. Chromosomes 1A, 2D, and 3D each have two linkage groups, and 7A and 7D each have three linkage groups (Appendix C; Table 3). The genetic map covers 3,567.30 cM, with the highest marker density observed on the B genome at an average of 0.66 cM between markers, and the lowest on the D genome at 1.71 cM (Table 3). Individual linkage groups also exhibited various lengths and densities (Table 3).

The 3,569 markers were successfully mapped to the IWGSC RefSeq v1.1, and the genetic map showed good collinearity with the physical map, except for chromosomes 2DL and 3BS, where inversion segments were detected (Appendix D).

Table 1 Basic statistics for the 'Nanjing 8611' and 'Ocoroni' F_6 (NJO) population in different environments

Trait[1)]	Environment[2)]	Parents		RILs		SD
		Nanjing 8611	Ocoroni	Mean	Min.–Max.	
FHB index (%)	2019-M	4.38	29.69	19.14	0.00–88.94	11.86
	2021-M	12.43	39.30	20.68	3.69–40.18	7.65
	BLUP-M	18.26	21.85	19.91	17.88–24.49	0.99
FHB severity (infected spikelets)	2020-NJ	3.80	6.40	9.14	1.80–15.60	2.68
	2021-NJ	3.70	18.60	12.39	1.80–22.00	4.97
	2022-NJ	7.00	9.50	8.13	1.00–20.00	3.70
	BLUP-NJ	6.68	11.04	10.16	5.92–14.91	1.95
DON (mg kg^{-1})	2019-M	5.00	11.60	6.66	1.65–19.50	2.74
	2021-M	4.45	11.75	6.63	1.47–13.25	2.10
	2020-NJ	6.15	4.48	24.57	1.53–94.03	19.21
	2021-NJ	13.71	–	34.18	3.47–85.99	16.23
	2022-NJ	31.36	13.66	28.01	3.61–85.67	18.12
	BLUP-M	5.95	8.06	6.49	5.20–9.22	0.56
	BLUP-NJ	23.41	22.54	8.95	18.39–50.90	6.20
PH (cm)	BLUP-M	93.16	89.50	94.61	73.00–110.26	7.46
DTH (d)	BLUP-M	65.19	60.88	61.66	53.80–74.77	3.65

[1)] FHB, Fusarium head blight; DON, deoxynivalenol; PH, plant height; DTH, days to heading.
[2)] M, CIMMYT, Mexico; NJ, Nanjing, Jiangsu Province, China; BLUP, best linear unbiased prediction.
–, data missing.

Table 2 Phenotypic correlation among traits in the 'Nanjing 8611' and 'Ocoroni' F_6 (NJO) population[1)]

Trait	FHB-M	FHB-NJ	DON-M	DON-NJ	DTH-M	PH-M
FHB-M	1					
FHB-NJ	0.260**	1				
DON-M	0.512**	0.152*	1			
DON-NJ	0.255**	0.635**	0.280**	1		
DTH-M	0.199**	–	0.311**	–	1	
PH-M	–0.121*	–	0.050	–	0.230**	1

[1)] M, CIMMYT, Mexico; NJ, Nanjing, Jiangsu Province, China; FHB, Fusarium head blight; DON, deoxynivalenol; DTH, days to heading; PH, plant height.
** and *, significances at P<0.01 and P<0.05, respectively. The analysis was conducted with the BLUP (best linear unbiased prediction) datasets.

3.3. QTL mapping results

A total of 13 QTLs were identified using BLUP datasets in the NJO population, being located on chromosomes 1B, 2D (4), 3B (4), 5D (2), 6D, and 7A (Table 4). Two of them, *QFhb.CIM-2D.1* and *QDon.CIM-3B.1/QFhb.CIM-3B.1*, were detected in both Mexico and Nanjing, with the resistance alleles from 'Ocoroni' and 'Nanjing 8611', respectively.

QFhb.CIM-2D.1, identified in two BLUP datasets, was located on chromosome 2DS (Fig. 2-A), explaining phenotypic variation of 14.06 and 14.29%, respectively (Table 4). It contributed to FHB and DON reductions of 4.28 and 2.41%, respectively, in Mexico, whereas it conferred more pronounced reductions in Nanjing, i.e., 14.81% for FHB and 7.52% for DON (Fig. 2-A). Having the same flanking markers, *QFhb.CIM-3B.1* and *QDon.CIM-3B.1* on chromosome 3BS were considered the same QTL, explaining 7.14 and 17.28% of phenotypic variation, respectively (Table 4). This QTL decreased FHB and DON by 5.45 and 7.10%, respectively, in Mexico, and by 7.53 and 12.94%, respectively, in Nanjing (Fig. 2-B). The remaining 10 QTLs detected only in one BLUP dataset explained 2.67 to 7.58% of the phenotypic variation (Table 4). Multi-environment traits detected four QTLs (LOD=8; Appendix E). *QFhb.CIM-2D.1* and *QDon.CIM-3B.1* were simultaneously detected by multi-environmental, further indicating that they were stable QTLs (Appendix E).

QTLs for DTH were identified on the long arms of chromosomes 5A and 5D, most likely corresponding to *Vrn-A1* and *Vrn-D1*, respectively, and those for PH were found on 2D and 4D, with the latter corresponding to *Rht-D1* (Table 4). None of these QTLs coincides with those for FHB/DON resistance.

3.4. Effects of *QFhb.CIM-2D.1* and *QDon.CIM-3B.1*

Compared with those with neither *QFhb.CIM-2D.1* nor *QDon.CIM-3B.1*, RILs with one of the two QTLs exhibited a significant reduction in FHB (Fig. 3-A) and DON (Fig. 3-B), and those with both QTLs always displayed the lowest infection. This trend applied to both Mexico and Nanjing (Fig. 3). Comparing RILs with *QFhb.CIM-2D.1* with those with *QDon.CIM-3B.1*, the latter generally outperformed the former, except for FHB-Nanjing (Fig. 3). Further analysis showed that FHB index and DON accumulation were not

Table 3 Marker statistics for the constructed map using wheat 55K SNP array

Chromosome	Group	Number of markers	Length (cM)	Marker density
1A	1	102	65.19	0.64
	2	25	16.65	0.67
1B	1	233	138.83	0.60
1D	1	101	164.83	1.63
2A	1	114	115.27	1.01
2B	1	221	89.96	0.41
2D	1	34	104.87	3.08
	2	203	98.46	0.49
3A	1	179	163.34	0.91
3B	1	234	234.48	1.00
3D	1	17	17.80	1.05
	2	103	213.66	2.07
4A	1	200	140.88	0.70
4B	1	117	88.66	0.76
4D	1	77	206.06	2.68
5A	1	242	165.56	0.68
5B	1	253	159.81	0.63
5D	1	150	200.52	1.34
6A	1	151	136.01	0.90
6B	1	174	90.70	0.52
6D	1	96	263.15	2.74
7A	1	24	19.79	0.82
	2	67	99.20	1.48
	3	131	132.17	1.01
7B	1	169	118.37	0.70
7D	1	35	84.53	2.42
	2	96	131.68	1.37
	3	21	106.87	5.09
A genomic	10	1,235	1,054.06	0.85
B genomic	7	1,401	920.81	0.66
D genomic	11	933	1,592.43	1.71
Total	28	3,569	3,567.30	1.00

affected by DTH and PH in this study (Appendix F).

3.5. Conditional QTL analysis

Conditional QTL analysis was performed to determine the influence of FHB on DON, using conditional phenotypic values for DON|FHB. No significant difference was detected for *QFhb.CIM-2D.1* (Fig. 4-A), whereas significant differences were observed for *QDon.CIM-3B.1*, in both Mexico and Nanjing (Fig. 4-B). This suggests that *QFhb.CIM-2D.1* decreases DON content by preventing FHB infection, whereas *QDon.CIM-3B.1* directly affects DON reduction.

3.6. Validation of the major QTLs *QFhb.CIM-2D.1* and *QDon.CIM-3B.1*

Two KASP markers were developed to validate the two major QTLs identified in this study. *KASP-1369*, tightly linked to *QFhb.CIM-2D.1*, clearly genotyped the DH and SWP populations into two allelic groups (Fig. 5). For DH, the two groups exhibited significant differences in FHB and DON, but not in DON|FHB, again suggesting that *QFhb.CIM-2D.1* has a direct effect on FHB and an indirect effect on DON (Fig. 5-A). For the SWP population, *QFhb.CIM-2D.1* significantly decreased FHB and DON by 18.30 and 11.84%, respectively, in Mexico, and significantly decreased DON by 19.30%, whereas no significant difference was identified for FHB in Nanjing, and DON|FHB in both Mexico and Nanjing (P<0.05, Fig. 5-B).

Although being located on chromosome 3BS, *QDon.CIM-3B.1* is different from *Fhb1*, because neither 'Nanjing 8611' nor 'Ocoroni' has the *Fhb1* gene (Fig. 6-A). The marker *KASP-8394*, tightly linked to *QDon.CIM-3B.1*, genotyped the SWP population into two allelic groups that exhibited significant differences in FHB of 20.07 and 28.76% in Mexico and

Table 4 Quantitative trait loci identified for the 'Nanjing 8611' and 'Ocoroni' F_6 (NJO) population[1)]

QTL	Dataset[2)]	Chromosome	Position (cM)	Left marker	Right marker	LOD	PVE (%)	Add
QFhb.CIM-1B.1	FHB-BLUP-NJ	1B	20	*AX-94704082*	*AX-94466584*	6.84	4.82	–0.50
QFhb.CIM-2D.1	FHB-BLUP-M	2D-1	56	*AX-109911369*	*AX-111600100*	7.91	14.06	0.34
	FHB-BLUP-NJ	2D-1	56	*AX-109911369*	*AX-111600100*	16.46	14.29	0.82
QFhb.CIM-2D.2	FHB-BLUP-NJ	2D-2	79	*AX-95121860*	*AX-179475456*	8.81	6.41	–0.58
QFhb.CIM-3B.1	FHB-BLUP-M	3B	49	*AX-95632884*	*AX-110938394*	9.46	13.73	–0.34
QFhb.CIM-3B.2	FHB-BLUP-M	3B	63	*AX-95209504*	*AX-179558357*	4.88	7.09	–0.24
QFhb.CIM-3B.3	FHB-BLUP-NJ	3B	69	*AX-179559075*	*AX-112287912*	6.09	4.21	–0.45
QFhb.CIM-5D.1	FHB-BLUP-NJ	5D	141	*AX-109210653*	*AX-111555981*	7.42	5.54	–0.51
QFhb.CIM-7A.1	FHB-BLUP-NJ	7A-1	123	*AX-179558859*	*AX-179560054*	3.94	2.67	0.36
QDon.CIM-2D.1	DON-BLUP-M	2D-2	8	*AX-108950311*	*AX-86176034*	3.53	4.85	–0.12
QDon.CIM-2D.2	DON-BLUP-NJ	2D-2	82	*AX-95090184*	*AX-112286275*	4.50	7.58	–1.79
QDon.CIM-3B.1	DON-BLUP-M	3B	49	*AX-95632884*	*AX-110938394*	11.85	17.28	–0.23
	DON-BLUP-NJ	3B	49	*AX-95632884*	*AX-110938394*	6.11	7.14	–1.73
QDon.CIM-5D.1	DON-BLUP-NJ	5D	147	*AX-110202211*	*AX-110717870*	3.84	4.57	–1.39
QDon.CIM-6D.1	DON-BLUP-NJ	6D	253	*AX-86174890*	*AX-109457259*	3.87	5.04	1.45
–	DTH-BLUP-M	5A	84	*AX-95631142*	*AX-179560340*	10.61	7.79	1.56
–	DTH-BLUP-M	5D	147	*AX-110202211*	*AX-110717870*	4.71	2.90	–0.94
–	PH-BLUP-M	2D-1	100	*AX-95682198*	*AX-94450228*	5.53	6.30	–2.14
–	PH-BLUP-M	4D	42	*AX-95659047*	*AX-110527441*	10.92	13.00	3.16

[1)] LOD, logarithm of odds; PVE, phenotypic variation explained; Add, additive effect at a QTL, where negative values indicate that 'Nanjing 8611' contributed the high phenotypic value, and positive values indicate that 'Ocoroni' contributed the high phenotypic value.

[2)] FHB, Fusarium head blight; DON, deoxynivalenol; DTH, days to heading; PH, plant height; BLUP, best linear unbiased prediction; NJ, Nanjing, Jiangsu Province, China; M, CIMMYT, Mexico.

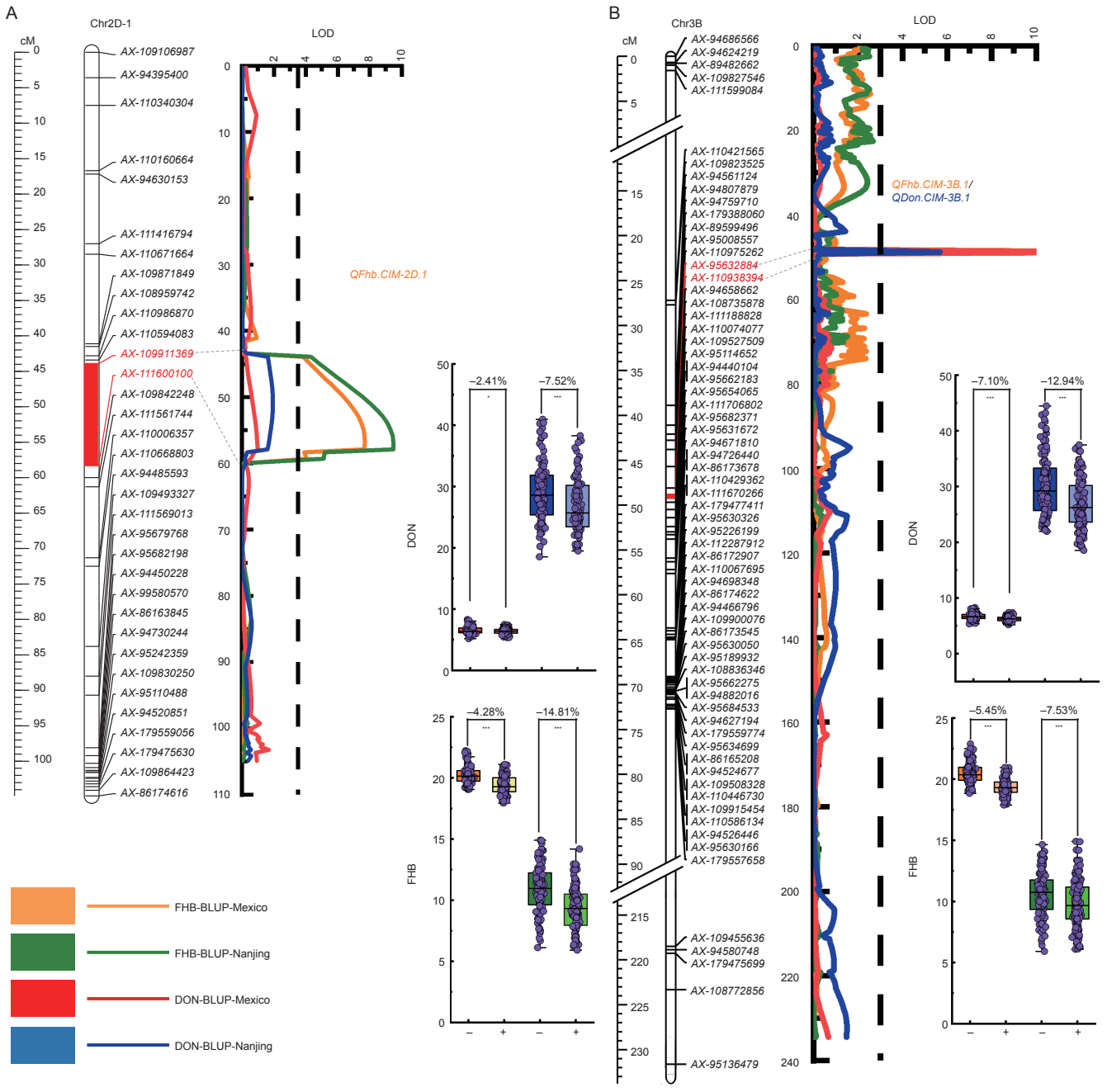


Fig. 2 Genetic map and QTL profile for *QFhb.CIM-2D.1* (A) and *QDon.CIM-3B.1* (B). Phenotypic differences between QTL groups are shown using box plots, where + and – represent RILs with and without the target QTL, respectively. *** and *, significances at $P<0.001$ and $P<0.05$, respectively. Differences in percentage between the compared groups are shown at the top of the charts.

Nanjing, respectively, with corresponding differences in DON of 23.25 and 61.26% (Fig. 6-A). *QFhb.CIM-2D.1* exhibited high frequencies of around 70% in both South and North American genotypes of the SWP population, whereas *QDon.CIM-3B.1* was far more frequent in the Asian genotypes (Fig. 6-B). It's worth noting that few North and South American genotypes carry *Fhb1*, whereas 33.82% of Asian genotypes do (Fig. 6-B). Genotypes with multiple QTLs demonstrated significantly reduced FHB and DON in the SWP population (Fig. 6-C).

3.7. Candidate gene analysis

Candidate genes were predicted based on the IWGSC RefSeq v2.1, and 178 and 41 (Appendix G) candidate genes were identified in the interval of *QFhb.CIM-2D.1* and *QDon.CIM-3B.1*, respectively. Additionally, the physical maps for *QFhb.CIM-2D.1* in IWGSC RefSeq v2.1 were in good agreement with those of Kenong 9204 and *Ae. tauschii* genomes (Appendices H and I). A similar observation was found for *QDon.CIM-3B.1* (Appendices H and J).

Based on the expression data of genes in the

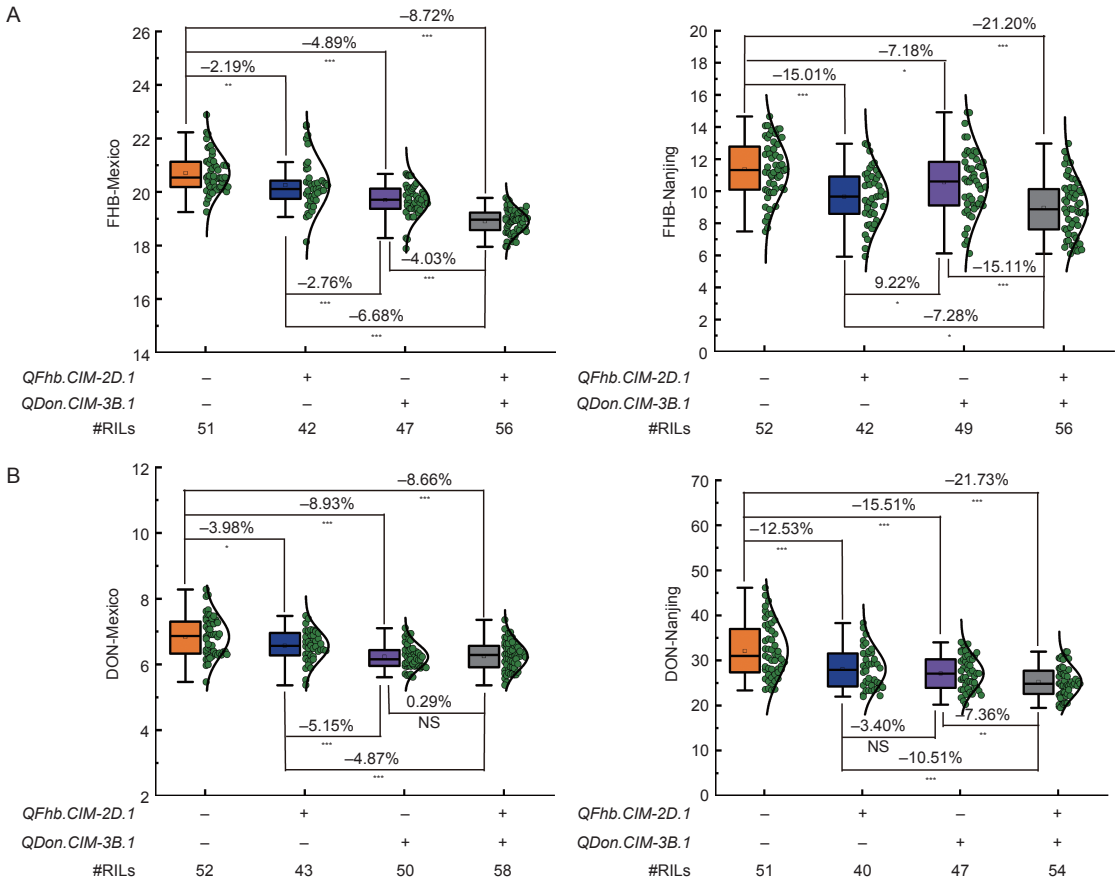


Fig. 3 Phenotypic effects of *QFhb.CIM-2D.1* and *QDon.CIM-3B.1* for Fusarium head blight (FHB) (A) on deoxynivalenol (DON) (B). + and – represent RILs with and without the target QTL, respectively. *** and *, significances at $P<0.001$ and $P<0.05$, respectively; NS, no significant difference. Differences in percentage between the compared groups are labeled at the top of the charts.

interval of *QFhb.CIM-2D.1*, *TraesCS2D02G050300* and *TraesCS2D02G057000* had the highest expression in spike and grain, respectively (Appendices K and L). As for *QDon.CIM-3B.1*, *TraesCS3B02G090200LC* and *TraesCS3B02G073600* had the highest expression in spike and grain, respectively (Appendices K and M). When temporal change is compared, *TraesCS2D02G052300*, *TraesCS2D02G053300*, and *TraesCS2D02G055600* for *QFhb.CIM-2D.1* were significantly induced at the later stages after inoculation (Appendices N and O), and *TraesCS3B02G073500* for *QDon.CIM-3B.1* also exhibited different expression levels across time points (Appendices O and P).

4. Discussion

4.1. Novelty of the two stable QTLs

Comparisons of the two stable QTLs detected in this study with those reported in previous studies were conducted by comparing their physical positions on the IWGSC RefSeq v2.1. *QFhb.CIM-2D.1* was located between 18,658,506 and 24,375,720 bp on chromosome 2DS (Appendix Q). It has been reported that *QFHB.caas-2D* was mapped in an interval between 14,570,019 and 24,7262,29 bp (Lv *et al.* 2014). Although the two QTLs showed a common interval mapping, the former conferred type II resistance, whereas the latter conferred type I resistance in our study. Besides, four other QTLs were also mapped in this interval with the tightly linked marker *Xgwm261* (Shen *et al.* 2003; Basnet *et al.* 2012). Among them, the QTL identified from 'Gamenya', which has the same genotype as 'Ocoroni', may be the same QTL as *QFhb.CIM-2D.1* in this study (Handa *et al.* 2008). The remaining three QTLs were different from *QFhb.CIM-2D.1* for the different genotypes between donor parents and 'Ocoroni'.

QDon.CIM-3B.1 was located between 53,878,431 and 55,697,103 bp on chromosome 3BS (Appendix R). Numerous previously identified QTLs were tightly linked to markers *Xgwm493*, *Xbarc147*, and *Xgwm533*, which coincide with those associated with the famous *Fhb1* gene, previously reported as an FHB-related loci (Prat *et al.* 2017; He *et al.* 2019; Ma *et al.* 2006; Serajazari *et al.* 2023). *Fhb1* was delimited to an approximately 300-kb region on contig Ctg0954b of Chinese Spring and *TaHRC*, a gene encoding a putative histidine-rich calcium-binding protein located between 2,460,534 and 2,461,361 bp, which has been reported as the key determinant of *Fhb1*-mediated resistance to FHB (Su *et al.* 2018). *QDon.CIM-3B.1* confers type III resistance, whereas *Fhb1* confers type II resistance; the *Fhb1* gene has been identified as absent in those two parents (Wu *et al.* 2022). Thus, *QDon.CIM-3B.1* could be a novel QTL.

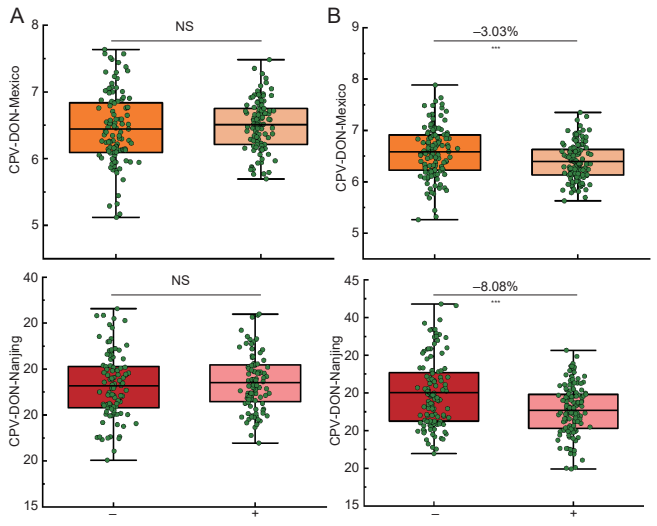


Fig. 4 Conditional QTL analysis for the influence of Fusarium head blight (FHB) on deoxynivalenol (DON) at *QFhb.CIM-2D.1* (A) and at *QDon.CIM-3B.1* (B). CPV, conditional phenotypic values (DON|FHB). ***, significance at $P<0.001$; NS, no significant difference. Differences in percentage between the compared groups are labeled at the top of the charts.

4.2. Resistance of 'Nanjing 8611' is conferred by multiple QTLs with moderate to minor phenotypic effects

'Nanjing 8611' has shown consistent resistance in previous evaluations in field experiments, greenhouse type II evaluations, as well as DON content (He *et al.* 2014; Osman *et al.* 2016; Wu *et al.* 2022).

Apart from *QDon.CIM-3B.1*, other resistance alleles contributed by 'Nanjing 8611' were all of minor effects, demonstrating that the high resistance of 'Nanjing 8611' was conferred by a range of QTLs with moderate to minor effects. This demonstrates that good FHB resistance is achievable *via* stacking multiple minor QTLs, which agrees with other researchers, e.g., stacking multiple minor QTLs can provide a high level of FHB resistance in a Chinese wheat landrace 'Haiyanzhong' (Cai *et al.* 2016).

The moderately susceptible parent 'Ocoroni' also contributed a major QTL *QFhb.CIM-2D.1*, which is not rare in genetic studies for FHB resistance, as reported by Basnet *et al.* (2012) and Shen *et al.* (2003). Because both parents contributed resistance alleles, transgressive segregation was observed, which justifies the strategy of developing FHB resistant varieties using parents with moderate resistance/susceptibility to FHB (Ma *et al.* 2019).

4.3. Collinearity between genetic and physical maps

The genetic map constructed in the current study has shown good collinearity with the physical map IWGSC RefSeq v1.1, suggesting that the former was robust and should be accurate in most chromosomal regions. Despite numerous markers being mapped, some intervals lacked markers, such as the terminal regions of chromosomes 4B and 6A. One reason could be the low levels of sequence polymorphism in the intervals between the parents of 'Nanjing 8611' and 'Ocoroni', and another could be the low marker coverage in those intervals, especially around centromere regions (Liu *et al.* 2018; Ren *et al.* 2018). Additionally, two intervals with chromosome inversion were identified on chromosomes 2DL and 3BS. However, whether these are real inversions or artifacts caused by different genetic backgrounds, they have little influence on the subsequent QTL mapping in this study (Mano *et al.* 2012; Liu *et al.* 2018; Ren *et al.* 2021).

4.4. Stacking of *QFhb.CIM-2D.1* and *QDon.CIM-3B.1*

FHB resistance is divided into different types that play distinct roles (Bai *et al.* 2018). *QFhb.CIM-2D.1* and *QDon.CIM-3B.1* as two major QTLs controlling FHB resistance were detected in the NJO population. Based on results from the conditional QTL analysis, it was shown that *QDon.CIM-3B.1* had a direct effect on DON reduction, whereas *QFhb.CIM-2D.1* had a direct effect on FHB resistance in point-inoculated experiments, indicating that they were responsible for Type III and Type II resistance, respectively. This is why we used *QDon.CIM-3B.1* instead of *QFhb.CIM-3B.1* when referring to this QTL in the present study. Although each QTL can significantly reduce the FHB index and DON content, the reduction became much more significant when both QTLs were present, clearly indicating the additive mode of the two QTLs. This is promising for their utilization in resistance breeding for FHB and DON, especially when they represent different resistance components and are independent of PH and DTH.

Fhb1 serves as an important resistance source utilized in wheat breeding to enhance FHB resistance. It has been widely used in winter wheat breeding, but less frequently used for spring wheat breeding in North and South America (Zhu *et al.* 2019b), which is consistent with our results in the SWP population. In Asian genotypes of SWP, *Fhb1* has a higher frequency and contributes significantly to FHB resistance, especially when combined with *QDon.CIM-3B.1* and *QFhb.CIM-2D.1*, implying the general association between a high number of QTL stacked with increased FHB resistance, which was also reported in other studies (Brar *et al.* 2019; Zhang *et al.* 2021; Hu *et al.* 2023).

A combination of the resistance QTLs and genes for breeding high yielding cultivars with improved FHB resistance appears highly promising in the future. It is worth noting that fewer than 40% of Asian genotypes carried the resistant allele of the QTL of *QFhb.CIM-2D.1* in the SWP population, and about 30% of *QFhb.CIM-2D.1* was underutilized in North and South America. Additionally, less than 30 and 5% of *QDon.CIM-3B.1* and *Fhb1*, respectively, were utilized in North and South America in this study. Therefore, we can increase attention to *QFhb.CIM-2D.1* in Asian, to *QDon.CIM-3B.1* and *Fhb1* in North and South America for subsequent FHB resistance breeding, respectively.

4.5. The candidate genes in the intervals of *QFhb.CIM-2D.1* and *QDon.CIM-3B.1*

QFhb.CIM-2D.1, located on chromosome 2DS, had 178 candidate genes in the mapping interval. Based on their expression with and without FHB infection, three higher-expression genes (*TraesCS2D02G052300*,

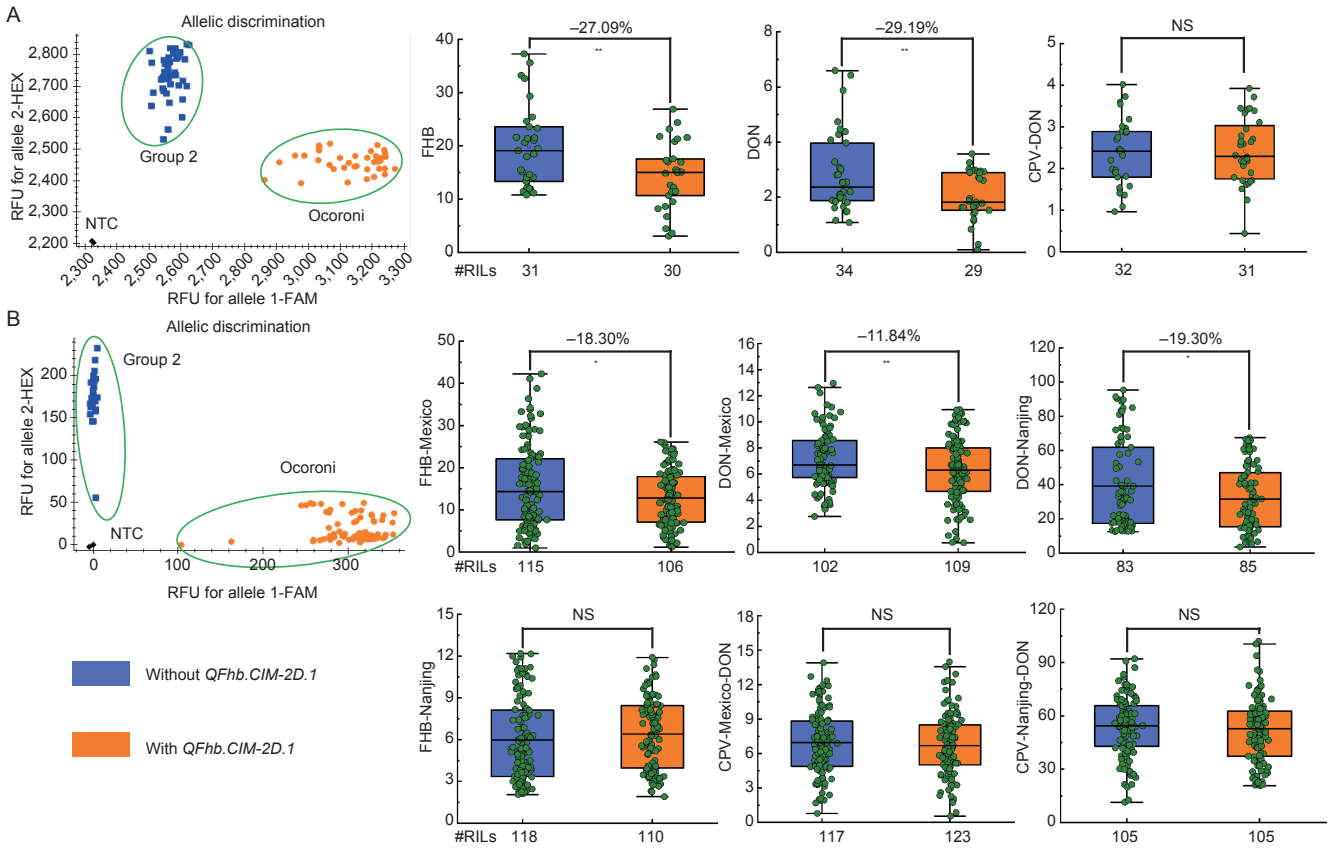


Fig. 5 Validation of *QFhb.CIM-2D.1* in the doubled haploid (DH) (A) and spring wheat panel (SWP) (B) populations. CPV, conditional phenotypic values (reduced deoxynivalenol (DON)|Fusarium head blight (FHB)). ** and *, significances at $P<0.01$ and $P<0.05$, respectively; NS, no significant difference. Differences in percentage between the two groups are labeled at the top of the charts.

TraesCS2D02G053300, and *TraesCS2D02G055600*) were identified. *TraesCS2D02G052300*, a homologous gene of *AT5G60900*, may be associated with different abiotic stresses (Mondal *et al.* 2021). *TraesCS2D02G055600* was associated with biotic and abiotic stress responses in rice (Yang *et al.* 2021) and *Arabidopsis* (Walley *et al.* 2007). *TraesCS2D02G053300* is a homologous gene of *LOC_Os04g13210*, which promotes the expression of defense genes and increases the resistance of rice plants to fungal and bacterial pathogens as well as herbivorous insects (Cheng *et al.* 2013; Liu *et al.* 2015). It is likely to be the candidate gene for *QFhb.CIM-2D.1*, which needs to be further verified *via* fine-mapping and expression analysis.

QDon.CIM-3B.1, located on chromosome 3BS, had 41 candidate genes in the mapping interval. Based on the expression analysis, four higher-expression genes (*TraesCS3B02G073500*, *TraesCS3B02G073600*, *TraesCS3B02G090200LC*, and *TraesCS3B02G090400LC*) were identified. *TraesCS3B02G073500* encodes a myosin-binding protein, which could serve as a binding domain for calmodulin and calmodulin-like myosin light chains and be connected with hydrolysis (Zhou *et al.* 2020). However, the expression abundance of the last three genes was not significantly changed after FHB inoculation in the present study. Thereby, we suspected that *TraesCS3B02G073500* may be the candidate gene for *QDon.CIM-3B.1*.

5. Conclusion

In this study, a RIL population with 269 F_6 lines derived from a cross between 'Nanjing 8611' and 'Ocoroni' was evaluated for FHB resistance with point inoculation in China and spray inoculation in Mexico. After genotyping the population with the wheat 55 K SNP array, a high-density genetic map was constructed, and 13 QTLs, including two major and stable QTLs (i.e., *QFhb.CIM-2D.1* and *QDon.CIM-3B.1*), were detected. Results from the conditional QTL analysis further concluded that *QFhb.CIM-2D.1* was associated with type II resistance and *QDon.CIM-3B.1* with type III resistance, and both were independent of PH and DTH. The two QTLs were successfully validated across different genetic populations using newly developed KASP markers. Because they exhibit an additive mode of action, their use in wheat breeding for FHB resistance is promising.

Acknowledgements

This research has been funded by the National Key R&D Program of China (2022YFD1400105), the International Scientific and Technological Cooperation Projects of Jiangsu Province, China (BZ2024043), the Seed Industry Revitalization Project of Jiangsu Province, China (JBGS2021006), and the Jiangsu Agricultural Science

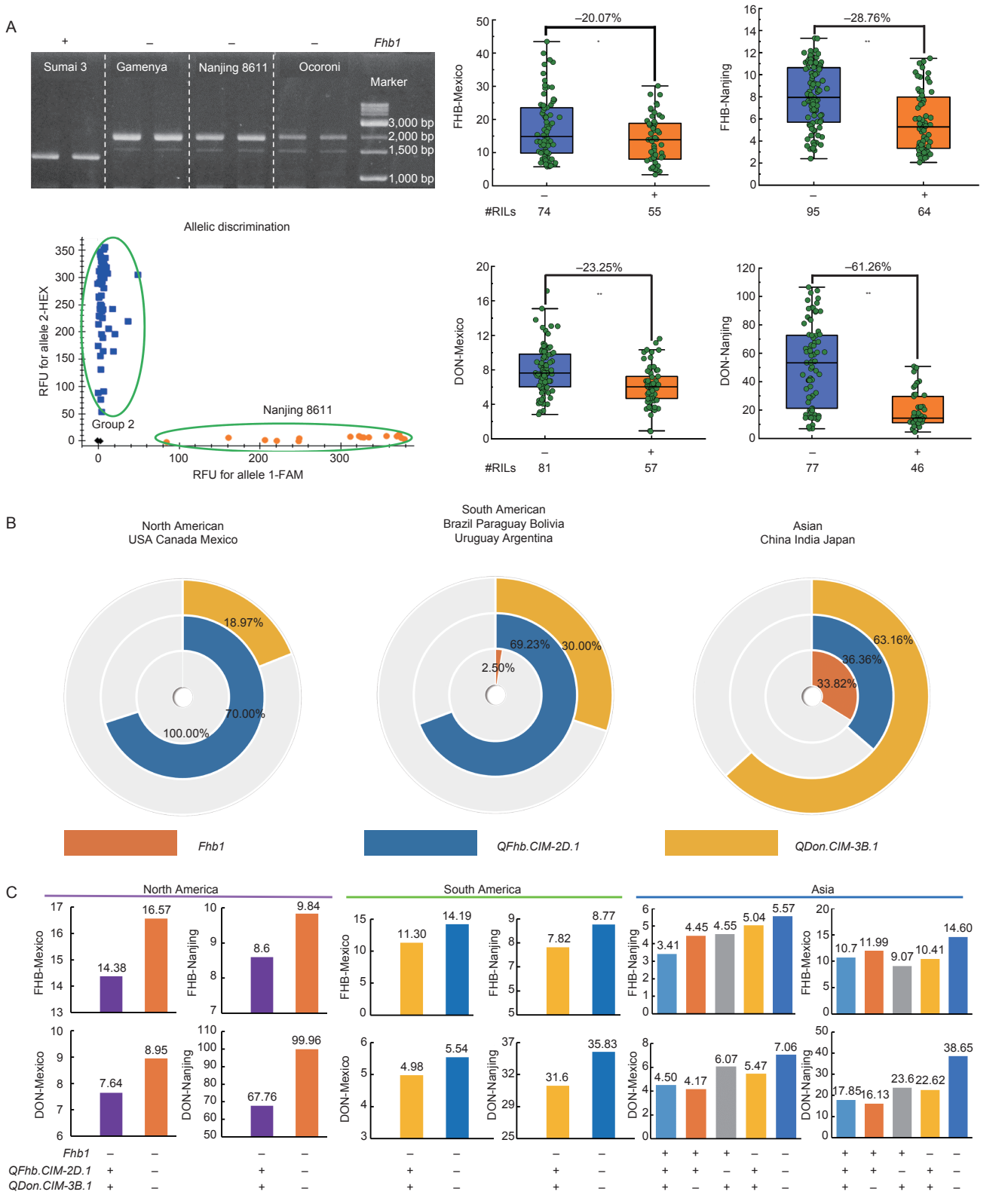


Fig. 6 Validation of *QDon.CIM-3B.1*. A, genotyping of the two parents with the *TaHRC* marker for *Fhb1* and testing the phenotypic effects of *QDon.CIM-3B.1* in the spring wheat panel (SWP) population with the newly designed marker *KASP-8394*. B, occurrence frequencies of *Fhb1*, *QFhb.CIM-2D.1*, and *QDon.CIM-3B.1* in the Asian, South and North American genotypes included in the SWP population. C, phenotypic effects of *QFhb.CIM-2D.1*, *QDon.CIM-3B.1*, and *Fhb1* in the SWP population.

and Technology Innovation Fund, China (CX (22)2005). Technical support from Francisco Lopez in field trials and Nerida Lozano in inoculum preparation for trials in Mexico is highly acknowledged. Technical support from Assistant Profs. Chang Li and Lixuan Yu in field trials in China is also well appreciated.

Declaration of competing interest

The authors declare that they have no conflict of interest.

Declaration of generative AI and AI-assisted technologies in the writing process

The authors declare that they did not use AI in the preparation and writing of this manuscript.

Appendices associated with this paper are available at https://doi.org/10.1016/j.jia.2024.12.021

References

Awika J M. 2011. Major cereal grains production and use around the world. *Advances in Cereal Science: Implications to Food Processing and Health Promotion*. Chapter 1. ACS Publications, Texas A&M University, USA. pp. 1–13.

Bai G, Su Z, Cai J. 2018. Wheat resistance to Fusarium head blight. *Canadian Journal of Plant Pathology*, **40**, 336–346.

Basnet B R, Glover K D, Ibrahim A M, Yen Y, Chao S. 2012. A QTL on chromosome 2DS of 'Sumai 3' increases susceptibility to Fusarium head blight in wheat. *Euphytica*, **186**, 91–101.

Brar G S, Brûlé-Babel A L, Ruan Y, Henriquez M A, Pozniak C J, Kutcher H R, Hucl P J. 2019. Genetic factors affecting Fusarium head blight resistance improvement from introgression of exotic Sumai 3 alleles (including *Fhb1*, *Fhb2*, and *Fhb5*) in hard red spring wheat. *BMC Plant Biology*, **19**, 179.

Cai J, Wang S, Li T, Zhang G, Bai G. 2016. Multiple minor QTLs are responsible for *Fusarium* head blight resistance in Chinese wheat landrace Haiyanzhong. *PLoS One*, **11**, e0163292.

Cainong J C, Bockus W W, Feng Y, Chen P, Qi L, Sehgal S K, Danilova T V, Koo D-H, Friebe B, Gill B S. 2015. Chromosome engineering, mapping, and transferring of resistance to *Fusarium* head blight disease from *Elymus tsukushiensis* into wheat. *Theoretical and Applied Genetics*, **128**, 1019–1027.

Chen A H, Islam T, Ma Z H. 2022. An integrated pest management program for managing *Fusarium* head blight disease in cereals. *Journal of Integrative Agriculture*, **21**, 3434–3444.

Cheng S, Zhang Y, Bie T, Gao D, Zhang B. 2012. Strategy of wheat breeding for scab resistance in China. In: *Proceedings of the 4th International Symposium on Fusarium head blight*, 23–26 Aug., 2012. Nanjing, China.

Cheng X, Wu Y, Guo J, Du B, Chen R, Zhu L, He G. 2013. A rice lectin receptor-like kinase that is involved in innate immune responses also contributes to seed germination. *The Plant Journal*, **76**, 687–698.

Cui F, Li J, Ding A, Zhao C, Wang L, Wang X, Li S, Bao Y, Li X, Feng D. 2011. Conditional QTL mapping for plant height with respect to the length of the spike and internode in two mapping populations of wheat. *Theoretical and Applied Genetics*, **122**, 1517–1536.

Gilsinger J, Kong L, Shen X, Ohm H. 2005. DNA markers associated with low *Fusarium* head blight incidence and narrow flower opening in wheat. *Theoretical and Applied Genetics*, **110**, 1218–1225.

Handa H, Namiki N, Xu D, Ban T. 2008. Dissecting of the FHB resistance QTL on the short arm of wheat chromosome 2D using a comparative genomic approach: From QTL to candidate gene. *Molecular Breeding*, **22**, 71–84.

He X, Dreisigacker S, Singh R P, Singh P K. 2019. Genetics for low correlation between *Fusarium* head blight disease and deoxynivalenol (DON) content in a bread wheat mapping population. *Theoretical and Applied Genetics*, **132**, 2401–2411.

He X, Lillemo M, Shi J, Wu J, Bjørnstad Å, Belova T, Dreisigacker S, Duveiller E, Singh P. 2016a. QTL characterization of *Fusarium* head blight resistance in CIMMYT bread wheat line Soru# 1. *PLoS One*, **11**, e0158052.

He X, Singh P K, Dreisigacker S, Singh S, Lillemo M, Duveiller E. 2016b. Dwarfing genes *Rht-B1b* and *Rht-D1b* are associated with both Type I FHB susceptibility and low anther extrusion in two bread wheat populations. *PLoS One*, **11**, e0162499.

He X, Singh P K, Duveiller E, Schlang N, Dreisigacker S, Singh R P. 2013. Identification and characterization of international Fusarium head blight screening nurseries of wheat at CIMMYT, Mexico. *European Journal of Plant Pathology*, **136**, 123–134.

He X, Singh P K, Schlang N, Duveiller E, Dreisigacker S, Payne T, He Z. 2014. Characterization of Chinese wheat germplasm for resistance to *Fusarium* head blight at CIMMYT, Mexico. *Euphytica*, **195**, 383–395.

Hu W J, Fu L P, Gao D R, Li D S, Liao S, Lu C B. 2023. Marker-assisted selection to pyramid *Fusarium* head blight resistance loci *Fhb1* and *Fhb2* in the high-quality soft wheat cultivar Yangmai 15. *Journal of Integrative Agriculture*, **22**, 360–370.

Li C, Tang H, Luo W, Zhang X, Mu Y, Deng M, Liu Y, Jiang Q, Chen G, Wang J, Qi P, Pu Z, Jiang Y, Wei Y, Zheng Y, Lan X, Ma J. 2020. A novel, validated, and plant height-independent QTL for spike extension length is associated with yield-related traits in wheat. *Theoretical and Applied Genetics*, **133**, 3381–3393.

Liu J, Luo W, Qin N, Ding P, Zhang H, Yang C, Mu Y, Tang H, Liu Y, Li W, Jiang Q, Chen G, Wei Y, Zheng Y, Liu C, Lan X, Ma J. 2018. A 55K SNP array-based genetic map and its utilization in QTL mapping for productive tiller number in common wheat. *Theoretical and Applied Genetics*, **131**, 2439–2450.

Liu Y, Wu H, Chen H, Liu Y, He J, Kang H, Sun Z, Pan G, Wang Q, Hu J, Zhou F, Zhou K, Zheng X, Ren Y, Chen L, Wang Y, Zhao Z, Lin Q, Wu F, Zhang X, *et al*. 2015. A gene cluster encoding lectin receptor kinases confers broad-spectrum and durable insect resistance in rice. *Nature Biotechnology*, **33**, 301–305.

Lv C, Song Y, Gao L, Yao Q, Zhou R, Xu R, Jia J. 2014. Integration of QTL detection and marker assisted selection for improving resistance to *Fusarium* head blight and important agronomic traits in wheat. *The Crop Journal*, **2**, 70–78.

Ma H, Zhang K, Gao L, Bai G, Chen H, Cai Z, Lu W. 2006. Quantitative trait loci for resistance to *Fusarium* head blight and deoxynivalenol accumulation in Wangshuibai wheat under field conditions. *Plant Pathology*, **55**, 739–745.

Ma H, Zhang X, Yao J, Cheng S. 2019. Breeding for the resistance to *Fusarium* head blight of wheat in China. *Frontiers of Agricultural Science and Engineering*, **6**, 251–264.

Ma S, Wang M, Wu J, Guo W, Chen Y, Li G, Wang Y, Shi W, Xia G, Fu D, Kang Z, Ni F. 2021. WheatOmics: A platform combining multiple omics data to accelerate functional genomics studies in wheat. *Molecular Plant*, **14**, 1965–1968.

Ma Z, Xie Q, Li G, Jia H, Zhou J, Kong Z, Li N, Yuan Y. 2020. Germplasms, genetics and genomics for better control of disastrous wheat *Fusarium* head blight. *Theoretical and Applied Genetics*, **133**, 1541–1568.

Mano Y, Omori F, Takeda K. 2012. Construction of intraspecific linkage maps, detection of a chromosome inversion, and mapping of QTL for constitutive root aerenchyma formation in the teosinte *Zea nicaraguensis*. *Molecular Breeding*, **29**, 137–146.

Mcintosh R. 1998. Breeding wheat for resistance to biotic stresses. *Euphytica*, **100**, 19–34.

Mcmullen M, Jones R, Gallenberg D. 1997. Scab of wheat and barley: A re-emerging disease of devastating impact. *Plant Disease*, **81**, 1340–1348.

Mengesha G G, Abebe S M, Mekonnen A A, Lera Z T, Shertore M M, Fedilu K B, Tadesse Y B, Tsakamo Y T, Issa B T, Cheleko D C. 2022. Effects of cultivar resistances and chemical seed treatments on *Fusarium* head blight and bread wheat yield-related parameters under field condition in southern Ethiopia. *Heliyon*, **8**, e08659.

Miller J D, Ewen M A. 1997. Toxic effects of deoxynivalenol on ribosomes and tissues of the spring wheat cultivars Frontana and Casavant. *Natural Toxins*, **5**, 234–237.

Mondal R, Biswas S, Srivastava A, Basu S, Trivedi M, Singh S K, Mishra Y. 2021. *In silico* analysis and expression profiling of S-domain receptor-like kinases (SD-RLKs) under different abiotic stresses in *Arabidopsis thaliana*. *BMC Genomics*, **22**, 1–15.

Van Ooijen J. 2009. MapQTL®6, Software for the mapping of quantitative trait loci in experimental populations of diploid species. Kyazma BV, Wageningen, Netherlands. p. 64.

Osman M, He X, Benedettelli S, Ali S, Singh P K. 2016. Identification of new sources of resistance to fungal leaf and head blight diseases of wheat. *European Journal of Plant Pathology*, **145**, 305–320.

Prat N, Guilbert C, Prah U, Wachter E, Steiner B, Langin T, Robert O, Buerstmayr H. 2017. QTL mapping of *Fusarium* head blight resistance in three related durum wheat populations. *Theoretical and Applied Genetics*, **130**, 13–27.

Qi L, Pumphrey M, Friebe B, Chen P, Gill B. 2008. Molecular cytogenetic characterization of alien introgressions with gene *Fhb3* for resistance to *Fusarium* head blight disease of wheat. *Theoretical*

and Applied Genetics, **117**, 1155–1166.
Ren T, Fan T, Chen S, Li C, Chen Y, Ou X, Jiang Q, Ren Z, Tan F, Luo P, Chen C, Li Z. 2021. Utilization of a Wheat 55K SNP array-derived high-density genetic map for high-resolution mapping of quantitative trait loci for important kernel-related traits in common wheat. *Theoretical and Applied Genetics*, **134**, 807–821.
Ren T, Hu Y, Tang Y, Li C, Yan B, Ren Z, Tan F, Tang Z, Fu S, Li Z. 2018. Utilization of a Wheat55K SNP array for mapping of major QTL for temporal expression of the tiller number. *Frontiers in Plant Science*, **9**, 333.
Serajazari M, Torkamaneh D, Gordon E, Lee E, Booker H, Pauls K P, Navabi A. 2023. Identification of *Fusarium* head blight resistance markers in a genome-wide association study of CIMMYT spring synthetic hexaploid derived wheat lines. *BMC Plant Biology*, **23**, 1–14.
Shen X, Zhou M, Lu W, Ohm H. 2003. Detection of Fusarium head blight resistance QTL in a wheat population using bulked segregant analysis. *Theoretical and Applied Genetics*, **106**, 1041–1047.
Shi X, Cui F, Han X, He Y, Zhao L, Zhang N, Zhang H, Zhu H, Liu Z, Ma B, Zheng S, Zhang W, Liu J, Fan X, Si Y, Tian S, Niu J, Wu H, Liu X, Chen Z, Meng D, Wang X, Song L, Sun L, Niu B, Xiao J, Li J, Ling H. 2022. Comparative genomic and transcriptomic analyses uncover the molecular basis of high nitrogen-use efficiency in the wheat cultivar Kenong 9204. *Molecular Plant*, **15**, 1440–1456.
Smith S, Kuehl R, Ray I, Hui R, Soleri D. 1998. Evaluation of simple methods for estimating broad-sense heritability in stands of randomly planted genotypes. *Crop Science*, **38**, 1125–1129.
Su Z, Jin S, Zhang D, Bai G. 2018. Development and validation of diagnostic markers for *Fhb1* region, a major QTL for *Fusarium* head blight resistance in wheat. *Theoretical and Applied Genetics*, **131**, 2371–2380.
Walley J W, Coughlan S, Hudson M E, Covington M F, Kaspi R, Banu G, Harmer S L, Dehesh K. 2007. Mechanical stress induces biotic and abiotic stress responses *via* a novel *cis*-element. *PLoS Genetics*, **3**, e172.
Wang H, Sun S, Ge W, Zhao L, Hou B, Wang K, Lyu Z, Chen L, Xu S, Guo J, Li M, Su P, Li X, Wang G, Bo C, Fang X, Zhuang W, Cheng X, Wu J, Dong L, *et al*. 2020. Horizontal gene transfer of *Fhb7* from fungus underlies *Fusarium* head blight resistance in wheat. *Science*, **368**, eaba5435.
Wu L, He X, He Y, Jiang P, Xu K, Zhang X, Singh P K. 2022. Genetic sources and loci for Fusarium head blight resistance in bread wheat. *Frontiers in Genetics*, **13**, 988264.
Xu Y, Li Y, Bian R, Zhang G, Fritz A K, Dong Y, Zhao L, Xu Y, Ghori N, Bernardo A, Amand P, Rupp J L S, Bruce M, Wang W, Akhunov E, Carver B, Bai G. 2023. Genetic architecture of quantitative trait loci (QTL) for FHB resistance and agronomic traits in a hard winter wheat population. *The Crop Journal*, **11**, 1836–1845.
Xue S, Xu F, Tang M, Zhou Y, Li G, An X, Lin F, Xu H, Jia H, Zhang L. 2011. Precise mapping *Fhb5*, a major QTL conditioning resistance to *Fusarium* infection in bread wheat (*Triticum aestivum* L.). *Theoretical and Applied Genetics*, **123**, 1055–1063.
Yang G, Fu S, Huang J, Li L, Long Y, Wei Q, Wang Z, Chen Z, Xia J. 2021. The tonoplast-localized transporter *OsABCC9* is involved in cadmium tolerance and accumulation in rice. *Plant Science*, **307**, 110894.
Zhang Y, Yang Z, Ma H, Huang L, Ding F, Du Y, Jia H, Li G, Kong Z, Ran C, Gu Z, Ma Z. 2021. Pyramiding of Fusarium head blight resistance quantitative trait loci, *Fhb1*, *Fhb4*, and *Fhb5*, in modern Chinese wheat cultivars. *Frontiers in Plant Science*, **12**, 694023.
Zheng T, Hua C, Li L, Sun Z, Yuan M, Bai G, Humphreys G, Li T. 2021. Integration of meta-QTL discovery with omics: Towards a molecular breeding platform for improving wheat resistance to *Fusarium* head blight. *The Crop Journal*, **9**, 739–749.
Zhou Y, Bai S, Li H, Sun G, Zhang D, Ma F, Zhao X, Nie F, Li J, Chen L. 2021. Introgressing the *Aegilops tauschii* genome into wheat as a basis for cereal improvement. *Nature Plants*, **7**, 774–786.
Zhou Y, Zhou X E, Gong Y, Zhu Y, Cao X, Brunzelle J S, Xu H E, Zhou M, Melcher K, Zhang F. 2020. Structural basis of *Fusarium* myosin I inhibition by phenamacril. *PLoS Pathogens*, **16**, e1008323.
Zhu J. 1995. Analysis of conditional genetic effects and variance components in developmental genetics. *Genetics*, **141**, 1633–1639.
Zhu T, Wang L, Rodriguez J C, Deal K R, Avni R, Distelfeld A, Mcguire P E, Dvorak J, Luo M C. 2019. Improved genome sequence of wild emmer wheat Zavitan with the aid of optical maps. *G3 — Genes, Genomes, Genetics*, **9**, 619–624.
Zhu Z, Hao Y, Mergoum M, Bai G, Humphreys G, Cloutier S, Xia X, He Z. 2019. Breeding wheat for resistance to Fusarium head blight in the Global North: China, USA, and Canada. *The Crop Journal*, **7**, 730–738.

Executive Editor-in-Chief Xueyong Zhang
Managing Editor Ning Wang